Damage tolerance analysis of ncf composite sandwich panels

Fredrik Edgren, Constantinos Soutis, Leif E. Asp

Damage tolerance analysis of ncf composite sandwich panels

Fredrik Edgren, Constantinos Soutis, Leif E. Asp

PII: S0266-3538(08)00166-8
DOI: 10.1016/j.compscitech.2008.04.041
Reference: CSTE 4056

To appear in: *Composites Science and Technology*

Received Date: 26 February 2008
Accepted Date: 11 April 2008

Please cite this article as: Edgren, F., Soutis, C., Asp, L.E., Damage tolerance analysis of ncf composite sandwich panels, *Composites Science and Technology* (2008), doi: 10.1016/j.compscitech.2008.04.041

DAMAGE TOLERANCE ANALYSIS OF NCF COMPOSITE SANDWICH PANELS

Fredrik Edgren[1], Constantinos Soutis[2] and Leif E. Asp[*1, 3]

[1]SICOMP AB, Box 104, 43122 Mölndal, Sweden

[2]The University of Sheffield, Aerospace Engineering, Mappin Street, Sheffield S1 3JD, UK

[3]Luleå University of Technology, Polymer Engineering, 971 87 Luleå, Sweden

ABSTRACT

This paper concerns development and validation of impact damage representations in carbon fibre Non-Crimp Fabric reinforced face sheets for damage tolerance analysis of sandwich panels loaded in compression. For this purpose, experimental data accompanied by fractographic observations have been employed to scrutinize numerical predictions by state-of-the-art notch strength models. As a result, equivalent hole representations of Visible Impact Damage (VID) and, more surprisingly, of the subtle Barely Visible Impact Damage (BVID) are recommended for reliable damage tolerance prediction of the compression after impact (CAI) load case for the investigated panels. This recommendation relies on the identification of the mechanisms controlling failure resulting in reliable damage tolerance predictions employing a linear cohesive zone model.

Keywords: **A**. Textile composites; **A**. Structural materials; **B**. Defects; **C**. Notch; **D**. Compression after impact (CAI)

1. INTRODUCTION

Non-crimp fabrics (NCF) are textile structures increasingly used as reinforcement in polymer composite materials. Compared to the traditionally used pre-impregnated tapes (prepregs) NCF offer an economically attractive alternative through *e.g.* the use of out-of-autoclave manufacturing processes [1]. In the NCF, layers of oriented fibre tows are stacked on top of each other and stitched together to give the fabric integrity. Through this procedure the fibre tow crimp is reduced compared to other textile alternatives (*e.g.* weaves). Reducing the crimp thus increases the in-plane mechanical properties compared to weaves. Also, the through thickness stitching may improve the out-of-plane properties of the laminates compared to traditional prepreg composites.

One major concern with laminated composites is the low compression after impact (CAI) strength. A lot of research has been devoted to this problem and several models have been developed for

prediction of the CAI strength. The majority of the CAI models developed for prepregs either consider delamination buckling and growth [2-4] or compressive failure due to stress concentrations in the vicinity of the impact damage. Models considering the impact damage as an equivalent hole has been used to predict the CAI strength of composite laminates. In these cases the rationale for modelling the impact damage as a hole is the presence of fibre fracture as part of the impact damage, see *e.g.* [5, 6]. Models have also been developed that treat the impact damage as a "soft inclusion", see *e.g.* [7]. There the properties of the material within the inclusion are degraded to simulate the behaviour of the impact damaged material.

A recent study on NCF composite laminates (as face sheets of sandwich panels) has shown CAI strength to be controlled by compression failure caused by stress concentrations [8]. In no case were delaminations observed to grow prior to failure of the panels. Kink-bands (narrow bands with micro buckled fibres, see *e.g.* [9]) were found to form in the impact damaged region prior to laminate failure. In fact, kink-bands were shown to develop already at approximately 50-70% of the failure load [8]. In another study [10] similar behaviour was found in monolithic NCF laminates. Kink-bands developed in a stable manner during gradual increase of compressive load. A suitable damage tolerance model for NCF composite laminates thus needs to consider this mode of failure and also account for the gradual development of damage during loading.

The objective of this study is to propose and validate a relatively simple damage representation in the impacted face sheet that could be employed in a damage tolerance analysis of CAI loaded NCF composite sandwich panels. The validity of the proposed damage representation with respect to damage tolerance is to be verified employing state-of-the-art notch strength models for analysis of panels tested in [8].

2. EXPERIMENTAL

2.1 Materials

In this study carbon fibre NCF composite laminates are utilised as face sheets of sandwich panels. The laminates were manufactured from T700 carbon fibre and Norpol DION 9500-501 Vinylester. The carbon fibre reinforcement was in the form of the biaxial NCF LT450 (0°/90°, 205 g/m^2 in each direction) and DB450 (+45°/-45°, 205 g/m^2 in each direction), manufactured by Devold AMT, Norway. In [8] two different panel configurations were investigated. Here, however, only one of these

* Corresponding author. E-mail: leif.asp@sicomp.se

configurations will be studied. This laminate lay-up was quasi-isotropic (QI), $[0°/90°/45°/-45°]_{s3}$, with a thickness of 5.4 mm. The sandwich core material used was 50 mm thick Divinycell H200 crosslinked PVC foam (density: 200 kg/m^3). The panels were manufactured by vacuum infusion of the vinylester into the dry reinforcement stacked on both sides of the core material.

The elastic properties of the laminate plies are presented in Table 1. The properties have been calculated using rule of mixtures and the Halpin-Tsai equations. Input data for the material constituents were taken from material data sheets from the material suppliers, these data are also found in an earlier study by Edgren and Asp [11]. The values in Table 1 have been calculated for a nominal laminate thickness of 5.4 mm. This thickness is divided into 24 plies of equal thickness. A knock-down factor $\eta = 0.85$ has been used to reduce the longitudinal stiffness E_L for the 0°- and 90°-plies. The corresponding knock-down factor for the ±45°-plies is 0.98. The knock-down factor is used to account for the average stiffness reduction due to fibre waviness. This waviness has been shown to be larger (amplitude) for the 0°/90° fabrics than for the ±45°-fabric, hence the difference in knock-down factor as described in reference [11]. The value of the knock-down factors are chosen to yield a correct overall structural response when compared with experimental values. For a thorough description of the concept with stiffness knock-down factor see reference [11]. The properties reported in Table 1 together with the laminate plate theory result in a Young's modulus for the quasi-isotropic laminate of 38.3 GPa.

Specimens for compression after impact testing were saw cut from a larger panel to a final dimension of approximately 300 mm × 300 mm. The two loaded sides of the panels were made plane and parallel by machining. A sketch of the panels is shown in Figure 1. In addition to the compression after impact panels, smaller panels with dimension 150 mm × 150 mm were manufactured, as described in [8]. In these panels a 50 mm diameter hole or a 50 mm (length) notch was machined in one of the panel skins. Both the hole and the notch were located centrally in the skin. The notch width was approximately 1.5 mm.

2.2 Mechanical Testing

Impact damage was inflicted to the (300 mm × 300 mm) sandwich panels using a drop weight rig. During the impact the panels were placed on a rigid steel plate and the impactor, with tip radius of 12.5 mm, was dropped onto the upper skin of the panel. The energy levels were varied by altering the drop height of the impactor. Two levels of damage were sought: *barely visible impact damage*, BVID, and *visible impact damage*, VID. In this case, an energy level of 100 J caused a BVID (residual dent

depth on the surface of the skins of 0.40 mm). No other damage was visible to the naked eye on the BVID panels. In contrast, the impacts causing VID left severe damage in the impacted skin. A hole of 18-20 mm in diameter was punched in the laminate with large amount of fibre fracture. The energy level employed to cause a VID was 250 J.

Each group of impacted panels, BVID and VID, contained four specimens for mechanical testing, totally 8 panels. For the BVID case, a fifth panel was impacted for characterisation of the impact damage by means of fractography. In addition, two panels each with hole and notch, totally four panels, were tested. The eight BVID and VID panels as well as the four holed and notched panels were all tested in uniaxial in-plane compression. The panels were placed between two rigid steel plates in a 2 MN press. The two unloaded edges of the panels were unsupported and free to move. Strains in the panel skins were monitored using strain gauges bonded onto the skins, see Figure 1. The panels were tested in compression under controlled displacement at a loading rate of 1 mm/min.

One panel from each type (BVID, VID, Hole, Notch), totally four panels, were subject to interrupted loading. For these panels the loading was stopped prior to final failure, typically at 80 – 90% of the average failure load for each damage and panel type. This procedure allowed for investigation of any damage developed in the skins prior to catastrophic failure by means of fractography.

2.3 Fractographic Analysis

All impacted panels were examined by ultrasonic C-scan after impact as well as after compression tests. The panel skins were also studied by optical microscopy of polished sections of pieces taken from impact damaged laminates.

From the interrupted test panels a small piece of the impacted laminate, at the point of impact, was cut out. These pieces were ground down and polished in the thickness direction. Through this procedure damage developed in each ply could be studied under the optical microscope. The BVID panel set aside after impact was examined in an optical stereo microscope after polishing from the side rather than from the top. The studied specimen was sectioned and polished generating detailed knowledge on the damage distribution in cross-sections through the impact damage. The observed damage were first drawn by hand onto a paper, and later manually transferred to a computer digital image.

3 MODELLING

The compressive strength of long, aligned carbon fibre-reinforced plastics (CFRP) is significantly lower (30%-40%) than the tensile strength of the material due to kink-band formation introduced by fibre instability (microbuckling). The earliest attempt to model this behaviour was given by Rosen [12]. Rosen predicted compressive strength based on an elastic fibre microbuckling and related buckling strength to the in-plane shear modulus of the composite (G_{12}). However, failure of modern filamentary composites occurs because of local non-linear matrix deformation at composite strains well below the yield strain of the matrix and elastic analysis substantially over-predicts compressive strength. Current models attribute the low compression strength and the mechanism of kink-band formation to initial fibre misalignment (waviness) but fibre and fibre-matrix interface properties may also play an important role [13]. For an elastic-perfectly plastic body Budiansky [14] showed that

$$\sigma = \frac{\tau_y \left[1 + \left(\frac{\sigma_{T_y}}{\tau_y} \right)^2 \tan^2 \beta \right]^{\frac{1}{2}}}{\phi_0 + \phi} \tag{1}$$

where τ_y and σ_{T_y} are the in-plane shear and transverse yield stresses of the composite, respectively. ϕ_0 is the assumed fibre misalignment angle in the kink-band, ϕ is the additional fibre rotation in the kink-band under a remote stress σ, and β is the band orientation angle, as shown in Figure 2. The critical stress $\sigma=\sigma_c$ is achieved at $\phi=0$ in equation (1). Once the failure stress of the 0°-ply is known, the compressive strength of any multidirectional (MD) 0°-dominated lay-up, σ_{un}, can be estimated simply by the Stiffness Ratio Method, equation (2)

$$\sigma_{un} = \frac{\sigma_c}{N E_1} \sum_{k=1}^{N} n^{(k)} E_{x\theta}^{(k)} \tag{2}$$

where σ_{un} is the unnotched laminate strength, σ_c is the strength of the 0° lamina, N is the total number of plies in the laminate, E_1 is the 0° ply stiffness in the fibre direction, n is the number of plies of a given orientation θ, and $E_{x\theta}$ is the modulus of a ply of orientation θ in the loading direction (x). Alternatively, a ply-by-ply failure analysis using the classical laminate theory and the maximum stress criterion could be performed, but the accuracy obtained by equation (2) is satisfactory.

The measured unnotched unidirectional compressive strength of the T700 carbon fibre NCF /vinyl ester material is 1020 MPa (from reference [15] adjusted for a nominal thickness of 5.4 mm) and together with the stiffness properties reported in Table 1, the unnotched compressive strength of the 5.4 mm thick $[0/90/+45/-45]_{s3}$ laminate is estimated by equation (2) equal to σ_{un}=328 MPa, which compares favourably with the measured strength of 364.4 MPa [15] (10% difference). The axial

Young's modulus of the NCF quasi-isotropic panel estimated by the laminate plate theory is 38.3 GPa (=E_{eff}) and the measured average failure strain of the unnotched laminate equal to 0.95%.

3.1 Notched strength

The compressive strength is further reduced by the presence of fastener holes and access cut-outs. Previous work by Soutis and co-workers [16, 17] have found that open holes cause more than 40% reduction in the strength of carbon fibre-epoxy and carbon fibre-PEEK laminates and that damage was initiated by fibre microbuckling in the 0° plies at the edge of the hole. This process has been modelled with varying degrees of sophistication. Early models assumed that failure occurred when the maximum stress in the structure equals the unnotched strength of the material (maximum stress criterion) underestimating considerably the residual strength of the composite. To account for the local 'ductility' of the material, researchers applied the average stress or point stress failure criteria. They introduced a characteristic length by assuming that fracture depends on attaining a critical stress (= unnotched strength) at a characteristic distance d_0 ahead of the notch or a critical average stress along a characteristic length a_0 ahead of the cutout. The characteristic distance is used as a free parameter to be fixed by best fitting the experimental data. Soutis *et al.* [16, 17] compared the damage zone (microbuckling surrounded by delamination) at the edge of the hole to a through-thickness line crack containing cohesive stresses. This equivalent crack is loaded on its faces by a normal traction, T, Figure 3, which decreases linearly with the crack closing displacement (CCD), $2v$.

It is assumed that the length of the equivalent crack λ represents the length of the microbuckle. When the remote load is increased the equivalent crack grows in length, thus representing microbuckle growth. The evolution of microbuckling is determined by requiring that the total stress intensity factor at the tip of the equivalent crack equals zero. When this condition is satisfied, stresses remain finite everywhere [17].

The equivalent crack length from the circular hole or notch is deduced as a function of remote stress σ^{∞}, *i.e.*,

$$\sigma^{\infty} = \sum_{i=1}^{n} \beta_i T_i = f\left(\lambda, \sigma_{un}, v_c, E, R, W\right) \tag{3}$$

detailed expressions for the functions β_i and T_i are given in reference [16]. Equation (3) gives an expression for the applied compressive stress as a function of microbuckling length, λ, unnotched strength, σ_{un}, critical crack closing displacement, v_c, laminate elastic properties, E and geometry (plate

width, W and hole radius, R). At a critical length, λ_{cr}, the remote stress σ^{∞} attains a maximum value, designated σ_{cr}, where catastrophic failure occurs. The model contains two unknown parameters, which can be measured independently or predicted analytically: the unnotched strength σ_{un} and the critical CCD v_c, which is related to the area G_C (fracture energy) under the assumed linear traction - crack displacement curve. For a linear softening cohesive zone law, Figure 3, the critical strain energy release rate G_C is given by

$$G_c = 2\int_0^{v_c} \sigma(v)\, dv = \sigma_{un}\, v_c \tag{4}$$

where v_c is the critical crack closing displacement on the crack traction- crack displacement curve, which is analogous to the crack opening displacement in tension. It is assumed that the fracture energy G_C represents the total energy per unit projected area dissipated by fibre microbuckling. Of course other damage modes may occur within this process zone like matrix plasticity in the off-axis plies and delamination, but the critical damage mechanism is the fibre kinking or microbuckling.

The value of the fracture energy release rate G_C can be obtained from a separate compressive kink propagation test, wherein the fracture toughness ($K_c = Y\sigma\sqrt{\pi a}$) of a laminate containing a sharpened long slit (=2a) is measured. For the NCF material examined here, a 150 mm long by 150 mm wide specimen with a 50 mm (=2a) long centre notch was tested in uniaxial compression that resulted to a K_C value of 60 MPa$\sqrt{}$m or G_C=94 kJ/m^2, but this may vary considerably since only one specimen was tested to failure; at least five well prepared specimens would be needed for valid results.

The alternative method [18] is to analytically estimate the critical crack closing displacement v_c, that appears in equation (4). Budiansky [14] in his microbuckling analysis for an idealised unidirectional lamina related the crack overlap displacement $2v_c$ that represents end-shortening δ in Figure 2 explicitly to fibre diameter and fibre volume fraction by [18].

$$2v_c = \frac{\pi d_f}{4}\left(\frac{V_f E_f}{2\tau_y}\right)^n \tag{5}$$

where d_f is the fibre diameter, E_f is the fibre elastic modulus and τ_y is the in-plane shear yield stress of the composite. For carbon fibre/epoxy system the exponent n=1/3. Jelf and Fleck [19] examined the results of six experimental studies that appeared in the composites literature for continuous fibrous systems and found that the kink band width w satisfies the following empirical expression

$$w = 0.68 d_f \left(\frac{V_f E_f}{\tau_y} \right)^{0.37} \quad (6)$$

The correction factor in equation (6) accounts for material imperfections (fibre waviness, voids, resin rich regions) and other damage modes in the form of matrix cracking and splitting that accompany the formation of fibre kinking/microbuckling, which are not accounted by the Budiansky model. Once the CCD and unnotched strength are known the fracture energy associated with fibre microbuckling (or fracture toughness $K_C = \sqrt{G_C E_{eff}}$) can be obtained from equation (4).

For the NCF CFRP system examined here, V_f=0.55, d_f=7μm, E_f=230 GPa and τ_y=40 MPa, which result to a $2v_c$=64 μm and hence G_C=11.66 kJ/m^2. The observed kink-band width w (=$2v_c$) from several optical micrographs that were obtained from sectioning studies was in the region of 200 to 220 μm that corresponds to a critical fracture energy G_C=36 to 44 kJ/m^2 (K_C=37 – 41 MPa√m).

It appears that for the NCF system a value of n=1/2 in equation (5) gives a more realistic value for the crack overlap displacement v_c=109 μm, which is approximately one half the NCF ply thickness and results to a fracture energy G_C=39.83 kJ/m^2 (K_C = 39.06 MPa√m). A kink band width ($2v_c$) of 218 μm is supported by the fractographic observations, see Figure 4. The fibre and ply waviness that is present in the NCF laminates together with the voids and resin rich regions that reduce substantially the axial stiffness, see section 2.1, lead to larger local displacements in the damage process zone and hence larger kind band width than the value predicted by equation (5), which could be considered as a lower bound value.

4. RESULTS AND DISCUSSION

4.1 Experimental Results

4.1.1 Impact damage

Details of the impact damage characteristics have been presented in an earlier paper by Edgren *et al*. [8]. Nevertheless, the results are briefly recapitulated describing the extent of damage formed in the sandwich face sheets during the impact. With this knowledge the extent of damage formed during the subsequent compression tests can be appreciated. The brief description is limited to damage in the face sheet, *i.e.* matrix cracks, delaminations and fibre fractures.

All impacted panels were investigated by means of ultrasonic C-scan. In Figure 5a, a C-scan image of a BVID panel is presented. Delaminations are clearly seen. The projected damage has an almost circular shape. The individual delaminations, however, are almost rectangular in shape, with the long boundaries of the delaminations straight. The delamination shape found in the VID (panel Figure 5b) is similar to that in the BVID case. The average diameter of the projected delamination damage is approximately 65 mm and 70 mm for the BVID and VID, respectively. As mentioned above, the diameter of the penetrated region was measured to be in the interval 18-20 mm. This is similar to the size of the region with overlapping delaminations through the thickness, in the BVID case reported in [8] and in scripted in Figure 5a.

The damage distribution in a panel with BVID was studied under a microscope. A section in the 90º-direction through the damaged laminate is presented in Figure 6. Some matrix cracks were observed in the laminate. The distribution of matrix cracks in the thickness direction tends to be cylindrical, rather than conical, in shape. In addition, the delaminations seen in the ultrasonic C-scan image, Figure 5a, were found also in the sectioned laminate in Figure 6. No other damage, *i.e.* no fibre fractures (shear-off or kink-bands), was found in the impact zone of the BVID panel. In contrast, the VID panels suffered from large amounts of fractured fibres at the impact site.

4.1.2 Compression test results and implications for modelling

In this section the results from the mechanical tests and fractographical studies are presented. Furthermore, the results and implications these have on the CAI modelling are discussed.

The measured failure strains from the compression tests are presented in Table 2 together with the computed notched strengths. It is clear from these results that the difference between BVID and VID types in these NCF panels is negligible with respect to failure strain (or stress).

It was concluded in [8] that formation and growth of kink-bands was the mechanism responsible for failure of the CAI panels as well as the open hole and notched panels. Furthermore, from the fractographic studies of the interrupted tests it was observed that kink-bands develop at loads significantly lower than load at failure. Kink-bands developed in several plies and in a relatively large region around the point of impact. Kink-bands found in panel skins subjected to interrupted tests are presented in Figure 7. This figure shows an in-plane view of all kink-bands found in the impacted panel skins. Each line in the figure represents a kink-band. Note that the kink-bands observed in the interrupted tests were not present after impact, as described above, but introduced as axial compressive

load was applied. It should also be noted that delaminations and residual dent formed during the impact event were found not to grow along or across the panel during the subsequent compressive loading. Consequently, observed post compression after impact damage development was limited to kink band formation.

The distribution of kink-bands in the thickness direction for the BVID panel (the same panel as presented in Figure 7a)) is presented in Figure 8. Kink-bands were found in 0°-plies as well as in 45°-plies [10]. The longest kink-band found was 22 mm.

In a previous study [10] indications were found that link the stable development of kink-bands during successive compressive loading to some of the features from the impact damage. Kink-bands were found to develop along delamination boundaries in plies adjacent to the delaminations. Several factors are likely to cause this behaviour. Local stress perturbations develop due to matrix cracks and delaminations. The stress field in the region around the residual dent also enhances the effects of the material discontinuities. Stresses due to bending and shear of the laminate develop and affect the local stress concentrations around the discontinuities. It is clear that the impact damage reduces panel stiffness locally (hence reduced lateral support to the 0° fibres) and promotes development of quite large kink-bands when loaded in axial compression.

Kink-bands in NCF laminates can also develop in a stable manner under other conditions than CAI. In [15] 25 mm wide unnotched NCF specimens were loaded in compression. The loading on some specimens was interrupted prior to failure and the specimens were subjected to fractographic studies. Kink-bands were found in single fibre tows. Presence of voids, ply or fibre waviness and local delaminations can trigger the initiation of fibre kinking or microbuckling (a fibre instability failure mode). However, kink-bands were not found to have grown to the large extent as found in the CAI panels where large delaminated areas were introduced during the impact loading.

Stable development of kink-bands were also found in the notched and open hole panels from interrupted tests. In the notched panel kink-bands forming a crack were found to extend 4.4 mm from the notch tip, see Figure 9. In the open hole panel kink-bands were found to extend only 1 mm. All of these findings together imply that kink-bands in single NCF plies are more prone to grow stably in the presence of stress concentrations or stress gradients.

In earlier studies [8] and [10] it was argued that the effects of the residual dent may be important to consider in impact damage tolerance analysis of these sandwich panels. In retrospect, this may be revalued. The results in Table 2 reveal that there is no difference in CAI strength for the BVID and the VID cases. A residual dent exists only for the BVID and cannot be utilised to explain the consistent results for the two cases of impact damage. Considering the amount of kink-bands found in panel skins in the interrupted tests (see Figure 7), an explanation for the results may be found. The BVID and VID panels feature similar amount of stable kink-band formation in the interrupted tests. This indicates that this damage (*i.e.* kink-bands) plays an important role in governing final panel failure and consequently the notch effect of these kink-bands does not differ to a large extent between the two impact damage cases. For this reason, consideration of the notch effect from these kink-bands will explain the consistent CAI performance for the BVID and VID damage cases.

The simplest method to model the effect of the stably formed kink-bands, illustrated in Figure 7, is through an equivalent damage model. The kink-bands developed during loading bear some resemblance with notches. Here, we propose to model the effects of impact damage employing an equivalent notch model. The consideration of an equivalent notch is motivated by observations of the strain field reported by Bull and Edgren [20] and Zenkert *et al.* [21]. In these works, digital speckle photography (DSP) was employed to monitor the strain field in the vicinity of the impact damage. The DSP results show that high strain levels occur, on the surface of the laminates, in a narrow, notch-like, band extending normal to the loading direction. A DSP plot from the same study as presented in [20] and [21] can be seen in Figure 10. This image shows the longitudinal strain (parallel to loading direction), on the surface of the sandwich laminate, the moment before laminate failure. The panel (the same panel as presented in Figure 1) has a BVID located central in the image (only a part of the panel skin is displayed in the figure). The dark region extending perpendicular to the loading direction in the centre of the image corresponds to compressive strain levels higher than approximately 1%. This region extends gradually outwards (to the left and right) during loading until final unstable failure. The damage formation in the surface layer of the impacted face during the final five seconds of a test of a BVID panel is depicted in Figure 11. At this stage of the test cracks (kinking fibres, seen as dark lines evolving in the upper part of the pictures) grow from the central region outwards, finally causing catastrophic failure of the panel.

The region of high strains, depicted in Figure 10, may be interpreted as an apparent notch with measurable dimensions. It should be noted that the BVID does not originally contain these sharp damage features, instead they (kink-bands in individual plies, see Figure 8) are formed during the

subsequent compression loading. As described earlier, damage characterisation of a BVID, prior to any post impact loading, reveals presence of three damage features; matrix cracks, delaminations and a residual dent. The projected damage area, as well as the residual dent, will be circular in shape –rather than notch shaped. These observations may direct the engineer to assign an equivalent hole model for CAI assessment. These observations imply damage tolerance models considering either an equivalent notch or equivalent hole to be assessed.

During compression loading of the impacted panels kink-bands of length up to 22 mm have been observed prior to catastrophic failure [8]. These kink-bands, illustrated in Figure 7, bear some physical resemblance with notches. Furthermore, the mechanism controlling failure of the impacted panels is identical to that controlling failure of the notched panel. Catastrophic failure of impacted panels is preceded by stable kink-band formation in individual plies. At some point one (the longest), or several, of these kink-bands grows unstable causing final failure of the panel. Results from damage tolerance analyses considering an equivalent notch or hole representation employing a linear cohesive zone model are presented in the following section. Based on these results recommendations for choice of damage representations in damage tolerance analyses of sandwich panels with impacted NCF composite face sheets are expressed.

4.2 Damage Tolerance Performance and Analysis

The compression after impact strength for the NCF panels is obtained from the Soutis *et al.* linear cohesive zone model [16, 17] described above, by replacing the impact damage with an equivalent notch or open hole [5, 22]. The input parameters in the model are the material elastic properties (E_L, E_T, G_{LT}, ν_{LT}), the unidirectional or multidirectional unnotched compressive strength, σ_{un}, and the fracture toughness K_C or critical fracture energy release rate G_C associated with fibre microbuckling. In Table 3 the predictions of the notched strength are based on K_C (or G_C) values obtained experimentally, while in Table 4, the G_C value obtained from equation (5) in conjunction with experimental observations and measurements of the fibre kink-band width is used.

The notched compressive strength for the 150 mm x 150 mm specimen with a 50 mm hole diameter or a 50 mm long centre notch (a/W=0.33), using σ_{un}=364.4 MPa and K_C= 60 MPa$\sqrt{m}$, are found equal to 175.10 MPa and 160.47 MPa, respectively with a critical microbuckling length of about 15.5 mm. The maximum stress failure criterion for the plate with the open hole would predict a strength of 91.1 MPa, which is 51% less than the measured value ($\sigma_{cr}^{\exp} = 188$ MPa), considerably underestimated, leading into a very conservative design and hence a heavier structure.

It should be noted that the K_C value used in the prediction presented in Table 3 are based on limited number of tests performed on a 150 mm x 150 mm specimen. Its value of 60 MPa√m appears to be quite high when compared with current continuous carbon fibre/epoxy or carbon fibre/PEEK systems examined in earlier studies [17] with values in the range of 40-50 MPa√m. Recent work by Bull and Edgren [20] that studied the compressive strength after impact of these particular NCF CFRP-foam core sandwich panels estimated that a K_C=47 MPa√m can reasonably predict the residual strength of the structure.

In Table 4, the notched compressive strength of the T700 NCF sandwich panels are predicted where the K_C value is obtained from equation (5) with n=0.5 (K_C=39 MPa√m). The attraction of this method is that the fracture energy associated with fibre microbuckling, G_C (or K_C) is entirely estimated from the material constituent properties and therefore reducing the mechanical tests required for characterising these sandwich structures.

The notched compressive strength for the 150 mm x 150 mm specimen with a 50 mm hole diameter or a 50 mm long centre notch, using σ_{un}=364.4 MPa and K_C= 39 MPa√m, are found equal to 140.7 MPa and 121.5 MPa, respectively with a critical microbuckling length of about 6 mm, which are approximately 20% lower than the measured residual strength values, giving a conservative estimate of the residual strength of these panels.

It should be noted from Tables 3 and 4 that when the impact damage is replaced with an equivalent circular hole the notched strength (*i.e.* CAI strength) is about 5-10% higher than that predicted by an equivalent centre notch. Also, the notched strength predictions are affected by the input values for σ_{un} and K_C. For instance, if the predicted unnotched strength by the Stiffness Ratio Method is used, σ_{un}=328 MPa and K_C= 39 MPa√m, then for the 300 mm x 300 mm specimen that contains an equivalent notch of 22 mm, is found that its notched strength is reduced from 182.46 MPa down to 174.2 MPa, while the critical buckling length is slightly increased to 9.96 mm. The more conservative notched strength predictions achieved with an equivalent notch model compared to an equivalent hole model, in addition to the experimental observations of stable kink-band formation and high strains in a band across the impact damage present guidance for the damage tolerance analysis. That is: damage tolerance analyses should best consider an equivalent notch representation of the damage, even of a panel containing a BVID (initial internal damage only matrix cracks and delaminations).

Figure 12 presents the effects of K_C and σ_{un} on the predicted notched strength for the examined 300 mm x 300 mm specimen that contains an equivalent centre notch/hole of 22 mm. In Figure 12a the notch sensitivity of the panel is shown to decrease (microbuckling critical length or damage tolerance increases) with increasing fracture toughness, as you would expect. As a consequence, the critical buckling length is found to increase with increased fracture toughness. A K_C of 30 MPa√m results in a critical microbuckling length of 4.8 mm whereas a fracture toughness of 60 MPa√m results in a critical microbuckling length of 17 mm.

The notched strength and the critical microbuckling length also depend on the assumed unnotched compressive strength. Since these stitched fabric systems demonstrate considerable variation in strength and stiffness properties due to fibre misalignment, layer waviness, resin rich regions and voids introduced during the manufacturing process, it is important to examine the sensitivity of the residual strength on the unnotched strength that is used as an input parameter in the cohesive zone model. In Figure 12b, σ_{un} varies while all the other properties and panel dimensions remain unchanged. The plots demonstrate that the notched strength increases with increasing unnotched strength. The analyses revealed that the critical microbuckling length is reduced for higher unnotched strengths, implying that stronger panels can tolerate less damage.

In Table 5, the stiffness, strength and fracture toughness properties of the T700 NCF $[0/90/\pm45]_{s3}$ laminate that could be used as input parameters in the linear cohesive zone model to predict the open hole/notch compressive or compressive after impact strengths are summarised. All properties in Table 5 can be measured or predicted from simple analytical models and be employed in damage tolerance analyses as discussed below.

4.2.1 Proposal of a reliable damage tolerance analysis procedure

Using the material properties in Table 5 in the linear softening cohesive zone model and assuming an equivalent notch or hole reliable damage tolerance predictions for the CAI loaded sandwich panels can be realised. In this section, procedures for such analyses of panels containing BVID and VID are given. The experimental observations reveal that panels containing both the blunt BVID, containing delaminations and matrix cracks only, and the VID penetrating the skin fail by the same mechanism, *i.e.* kink-band formation. Both panels with a BVID and a VID fail catastrophically only after stable formation of a significant amount of kink bands. In the BVID case, this is resulting in a highly strained band crossing the impact centre point.

To model the damage tolerance one has to choose a simplistic damage representation. As discussed above, both an equivalent hole as well as an equivalent centre notch may be employed to successfully analyse the panels under consideration in this paper (only 5-10% difference between the two damage configurations). The experimental observations support the choice of an equivalent notch model, even for the BVID case. Such a choice is however hampered by the difficulty in the required selection of notch length. That is, the notch length must be selected on the basis of the characteristics of the BVID – lacking the presence of the critical kink bands when monitored. For this reason, a procedure only taking into account the damage accessible to the NDT-engineer is suggested. For the VID it is suggested that the damage is modelled as an equivalent open hole with a diameter equal to that of the penetrated region, illustrated in Figure 5b. Modelling the VID case with a hole diameter of 20 mm a residual compressive strength of 187 MPa is estimated that is less than 1% lower than the measured value, Table 2. The notch strength versus hole diameter for the equivalent hole model is depicted in Figure 13. A smaller size hole would result in a higher strength and vice versa, as illustrated in Figure 13. The equivalent hole size for the VID panel corresponds to the actual hole size introduced during the 250 J impact that perforated the sandwich plate, Fig. 5b.

In the BVID case the diameter of the delaminated region (projection) is approximately 65 mm but there are no broken fibres, no perforation, and therefore selection of a smaller size hole is advisable. The experimental observations implied that the adjacent delamination boarders promote kink band formation; the stress concentration at the boundary and the reduced local stiffness due to damage resulting into less lateral support provided to the 0° load carrying fibres promote these fibres to buckle (a fibre instability mode) at a lower applied load. For this reason, it is suggested that an equivalent hole diameter equal to the diameter of the region with overlapping delaminations, see Figure 5a and 6, is assumed. In the case of the BVID, the diameter of region with overlapping delaminations was 17 mm. According to Table 4, this results in a predicted CAI strength (residual strength) of 194.9 MPa. This is overestimating the CAI strength of the BVID panels by less than 6%, which is well within the expected scatter in tests. A larger equivalent hole diameter would result in to a more conservative value for the residual strength. From this point, conservatism in CAI strength predictions may be added further (5-10 percent) in both cases, replacing the equivalent hole with an equivalent notch of the same length as the diameter of the replaced hole.

The results presented in Table 4 could help the designer to determine an appropriate equivalent hole size and therefore a safety factor for a reliable damage tolerant design of these NCF composite sandwich panels.

5 CONCLUSIONS

Impact damage tolerance analyses of any composite material structure require simple (easy to use and measure), yet representative, characteristics of the damage in the employed models. That is, damage features strongly influencing the neighbouring stress field and damage mechanisms controlling failure must be captured by the selected damage representation. Impact damage in composite materials always contains matrix cracks, which are accompanied by delaminations, residual dent and fibre fractures as the severity of the impact increases. The call for simplification of the damage representation stems from this complexity in damage features. In fact, given the complexity of any impact damage it is hard to imagine that all its detail can ever be considered in an impact damage tolerance analysis. This paper addresses development and validation of sound impact damage representations in NCF reinforced CFRP skins of impacted sandwich structures loaded in compression. For this purpose, a state-of-the-art damage tolerance model considering a linear cohesive zone model is employed.

The experimental results reveal that the panels with a penetrated (VID) face sheet fail at similar load levels as panels with more subtle damage (BVID). In addition, thorough fractographic analysis of both types of panels subjected to interrupting compressive loading revealed fibre microbuckling (kink-bands) to control their strength. For both damage types, a stable phase of kink-band formation preceded catastrophic failure (due to unstable kink-band crack growth). Moreover, the experimental results suggest the kink-bands forming during compressive loading, subsequent to the impact event, to be best represented by a single equivalent notch. Results from damage tolerance modelling support this finding. However, moving from the equivalent notch representation of the damage to an equivalent open hole model inflicts only a five to ten percent change in the predicted notch strength. This observation, in addition to the difficulty connected with the determination of a critical notch length results in a recommendation to consider an equivalent hole of a diameter equal to the zone containing overlapping delamination or the diameter of the penetration for the BVID and VID cases, respectively. These parameters can be monitored and measured during regular ultrasonic C-scans or visual inspections.

6 REFERENCES

1. Avila-Dominguez, R., "NCF processability and performance –A literature review-", DERA/MSS/MSMA2/WP003564, Farnborough, UK, 2000.
2. Chai H., Babcock C.D., Knauss W.G.., "One-dimensional modelling of failure in laminated plates by delamination buckling". Int. J. Solids Struct. 1981;17: 1069-1083.

3. Whitcomb J.D.," Finite element analysis of instability related delamination growth". J. Comp. Mater. 1981;15: 403-426.
4. Nilsson K-F., Asp L.E., Alpman J.E., Nystedt L., "Delamination buckling and growth for delaminations at different depths in a slender composite panel". Int. J. of Solids Struct. 2001;38: 3039-3073.
5. Soutis C., Curtis P.T., "Prediction of the post-impact compressive strength of CFRP laminated composites". Compos. Sci. Technol. 1996;56: 677-684.
6. Hawyes V.J., Curtis P.T. and Soutis C., "Effect of impact damage on the compressive response of composite laminates", Compos. A, 2001;32: 1263-1270.
7. Nyman T., "Fatigue and residual strength of composite aircraft structures". Doctoral thesis. Report 99-26, Royal Institute of Technology, Stockholm, Sweden, ISSN0280-4646. 1999.
8. Edgren F., Asp L.E. and Bull P.H., "Compressive failure of impacted NCF composite sandwich panels – Characterisation of the failure process," J. Compos. Mater. 2004;38(6): 495 - 514.
9. Fleck N.A., "Compressive failure of fiber composites". Advances in Applied Mechanics. Academic Press. New York. 1997;33: 43-117.
10. Edgren F., "Compressive failure of NCF composites" Proc. American Society for Composites Twentieth Technical Conference., Paper No 26, September 7-9, 2005, Drexel University, Philadelphia, USA.
11. Edgren F. and Asp L.E., "Approximate analytical constitutive model for non-crimp fabric composites," Compos. A, 2005;36: 173-81.
12. Rosen, B.W. (1965). "Mechanics of composites strengthening". In: Fiber Composite Materials. American Society of Metals Seminar, Ohio: ASM, 1965, 37-75 (Chapter 3).
13. Soutis, C. "Compressive strength of unidirectional composites: measurement and prediction". ASTM-STP1242, 1997;13: 168-176.
14. Budiansky, B. "Micromechanics". Computers and Structures, 1983;16(1): 3-12.
15. Edgren F., Asp L. E. and Joffe R. "Failure of NCF composites subjected to combined compression and shear loading", Compos. Sci. Technol., 2006;66: 2865-2877.
16. Soutis, C., Fleck, N.A. and Smith, P.A.. "Failure prediction technique for compression loaded carbon fibre-epoxy laminate with an open hole". J. Comp. Mat., 1991:25: 1476-1498.
17. Soutis, C., Curtis, P.T. and Fleck, N.A. "Compressive failure of notched carbon fibre composites". *Proc. R. Soc. Lond. A*, 1993;440:, 241-256.
18. Soutis, C. and Curtis, P.T.. "A method for predicting the fracture toughness of CFRP laminates failing by fibre microbuckling". Compos A, 2000;31(7): 733-740.

19. Jelf, P.M. and Fleck, N.A. “Compression failure mechanisms in unidirectional composites”. *J. Mat. Sci.*, 1994;29: 3080-85.

20. Bull P.H. and Edgren F., "Compressive strength after impact of CFRP-foam core sandwich panels in marine applications", Compos. B, 2004;35: 535-541.

21. Zenkert D., Shipsha A., Bull P. and Hayman B., "Damage tolerance assessment of composite sandwich panels with localised damage", Compos. Sci. Technol. 2005;65: 2597-2611.

22. Curtis, P.T., Hawyes, V.J. and Soutis, C. “Effect of impact damage on the compressive response of composite laminates”. Compos A, 2001**;**32(9): 1263-1270.

TABLES

Table 1. Elastic material properties of the laminae (analytical estimates).

Property:	**0°-, 90°-plies**	**±45°-plies**	**Core**
E_L [GPa]	100.3	115.6	0.310
E_T [GPa]	7.6	7.6	-
G_{LT} [GPa]	2.9	2.9	-
G_{TT} [GPa]	2.9	2.9	-
ν_{LT} [-]	0.36	0.36	0.3
ν_{TT} [-]	0.31	0.31	-

Table 2. Strain to failure for compression loaded panels (standard deviations within brackets).

Damage type	**Failure strain [%]**	**Notched strength [MPa]**
BVID	-0.48 (0.01)	184
VID	-0.49 (0.04)	188
Hole	-0.49 (-)	188
Notch	-0.42 (-)	161

Note: Unnotched compressive strength, σ_{un}=364.4 MPa

Table 3. Predicted notched compressive strength of NCF sandwich panels

2a mm	a/W	σ_n^{OH} MPa	λ_{cr}^{OH} mm	σ_n^{Notch} MPa	λ_{cr}^{Notch} mm
2.5	0.0083	335.81	15.51	331.79	15.83
5	0.017	315.47	16.46	310.37	16.13
10	0.033	283.53	17.47	277.92	16.56
15	0.05	260.18	18.07	254.31	16.85
20	0.067	242.76	18.34	236.30	17.04
22	0.073	236.95	18.40	230.18	17.10
25	0.083	229.17	18.42	221.90	17.17
30	0.1	218.18	18.36	209.99	17.27
40	0.133	201.29	18.02	191.13	17.39
50	0.166	188.61	17.48	176.56	17.45
60	0.2	178.40	16.83	164.67	17.47

Notes: L=W=300 mm, t=5.4 mm, σ_{un}=364.4 MPa, G_C=94 kJ/m^2 (K_C= 60 MPa$\sqrt{m}$),
σ_n^{OH} = Open Hole compressive strength
σ_n^{Notch} = centre notch compressive strength

Table 4. Predicted notched compressive strength of NCF sandwich panels

2a mm	a/W	σ_n^{OH} MPa	λ_{cr}^{OH} mm	σ_n^{Notch} MPa	λ_{cr}^{Notch} mm
2.5	0.0083	307.0	7.43	302.15	7.09
5	0.017	269.93	7.89	266.27	7.35
10	0.033	225.75	8.28	223.20	7.64
15	0.05	201.64	8.25	197.46	7.79
17	0.056	194.9	8.20	189.71	7.84
20	0.067	186.81	8.06	179.88	7.88
22	0.073	182.46	7.95	174.27	7.91
25	0.083	177.06	7.77	166.91	7.94
30	0.1	170.0	7.44	156.46	7.98
40	0.133	159.86	6.75	140.6	8.02
50	0.166	152.30	6.12	127.46	8.04
60	0.2	145.91	5.56	117.23	8.04

Notes: L=W=300 mm, t=5.4 mm, σ_{un}=364.4 MPa, G_C=39.8 kJ/m^2 (K_C= 39 MPa$\sqrt{m}$)

Table 5 Face sheet engineering elastic constants and fracture toughness parameters

Material	E_x GPa	E_y GPa	G_{xy} GPa	ν_{xy}	σ_{un} MPa	K_C MPa$\sqrt{m}$	G_c kJ/m^2	v_c μm
T700/Ep	38.3	38.3	14.4	0.33	364.4	39	39.8	109

FIGURES

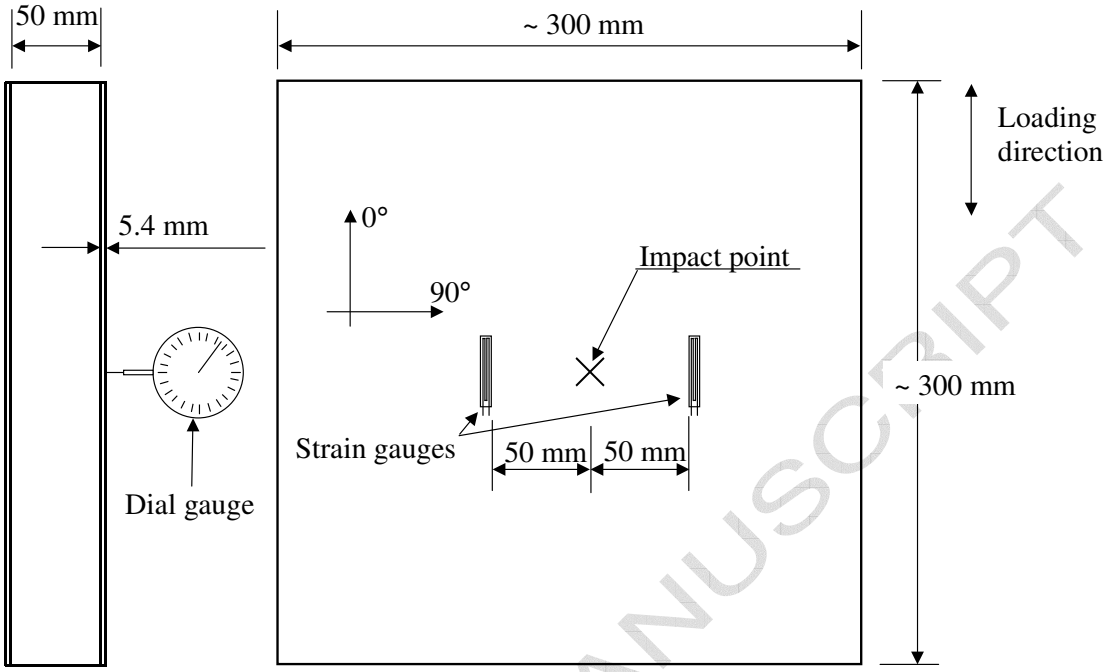

Figure 1. Dimensions of sandwich panels and positions of strain gauges and dial gauges.

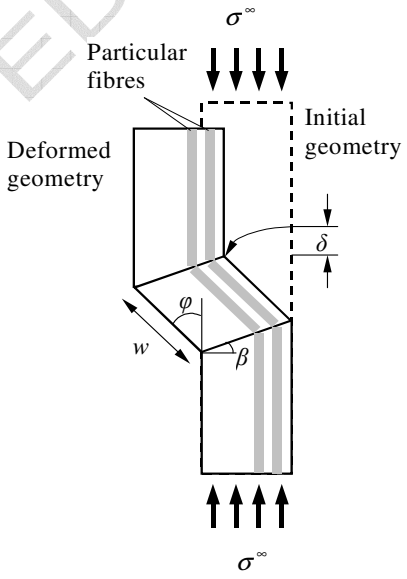

Figure 2 A schematic illustrating the specimen deformed geometry and the fibre kink-band geometry

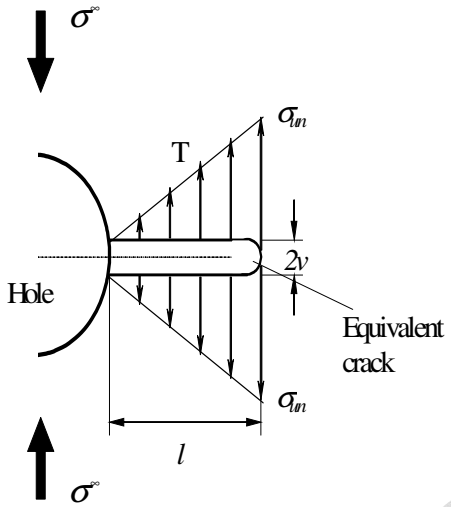

Figure 3 Damage zone is modelled as a line crack, loaded on its faces by a normal traction, *T*

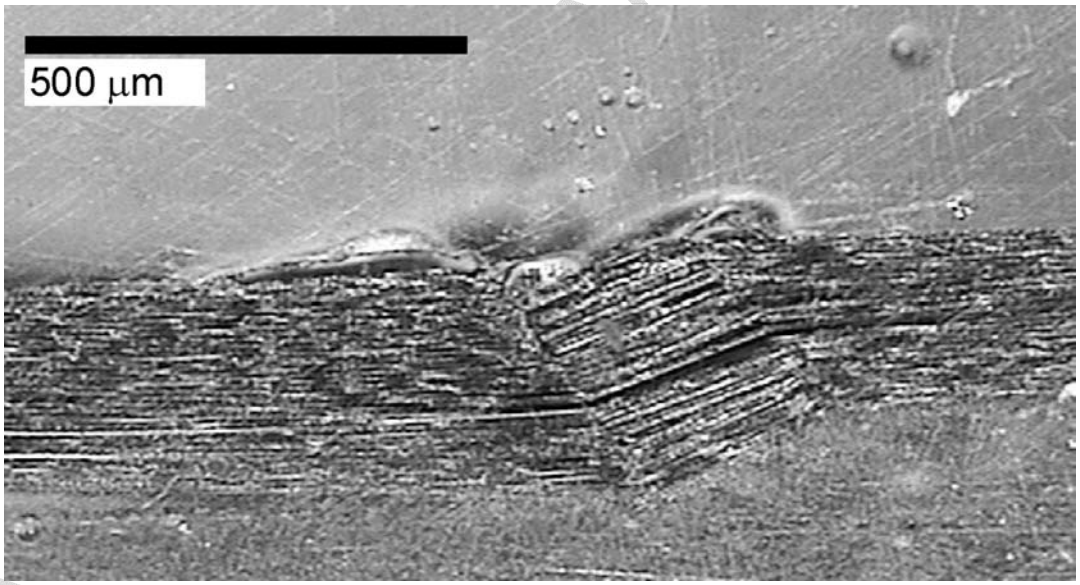

Figure 4 Kink-band found in an unnotched NCF composite loaded in compression, from [15].

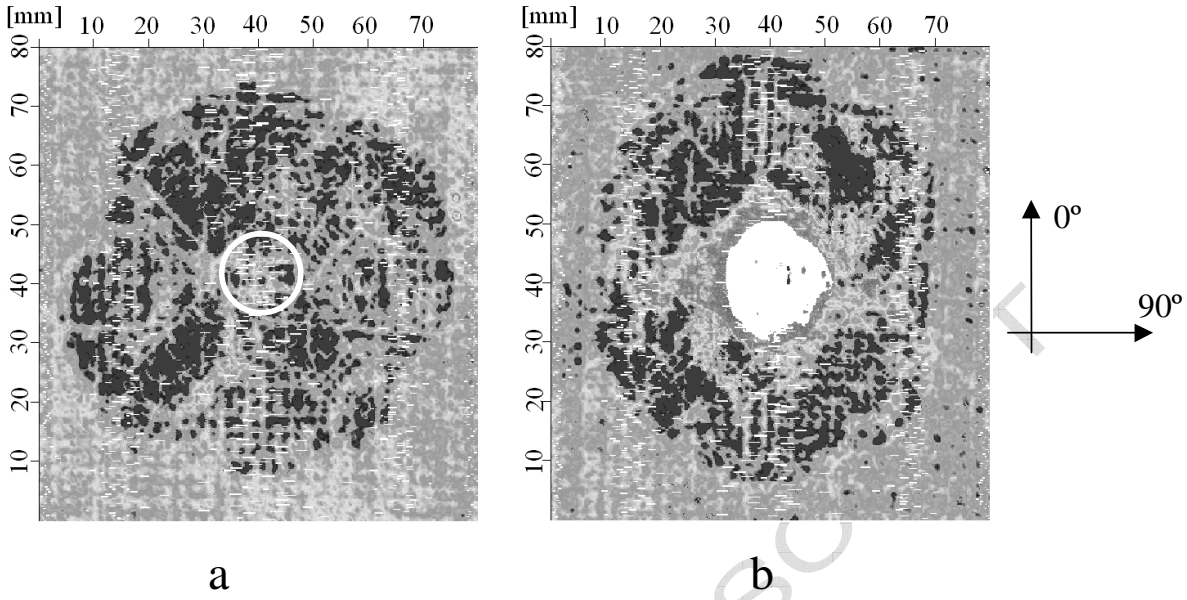

Figure 5. Ultrasonic C-scan images of a) BVID panel (100 J), in scripted circle indicate region of overlapping delaminations (Ø17 mm), and b) VID panel (250 J impact).

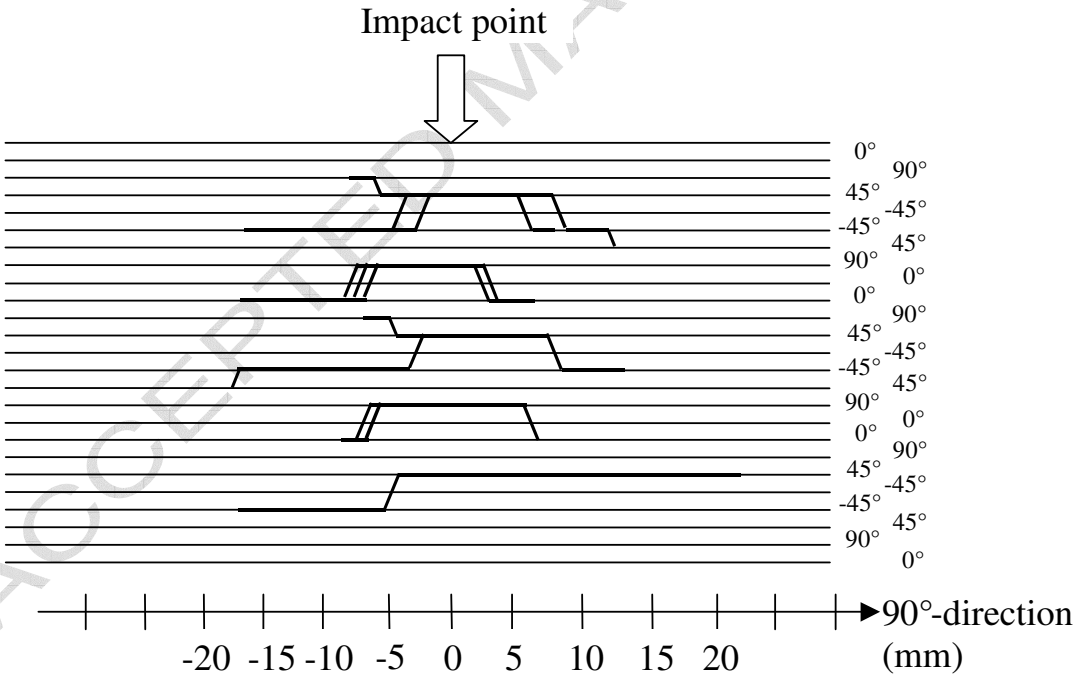

Figure 6. Schematic description of the damage features in the BVID.

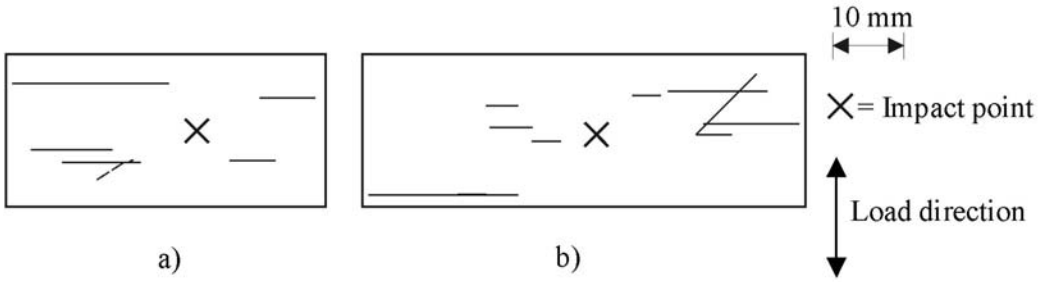

Figure 7. Kink-bands found in impact damaged face sheets after interrupted loading: a) BVID and b) VID (sketch does not represent full width of panel).

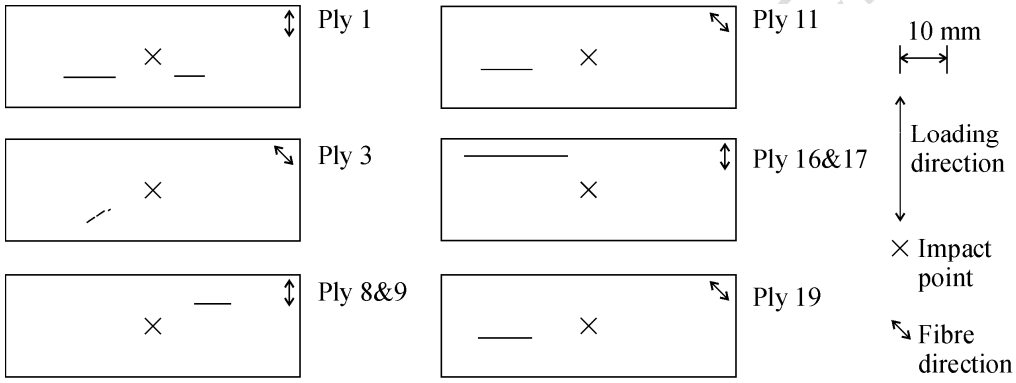

Figure 8. Kinkbands found in panel with BVID after interrupted compressive loading (sketch does not represent full width of panel).

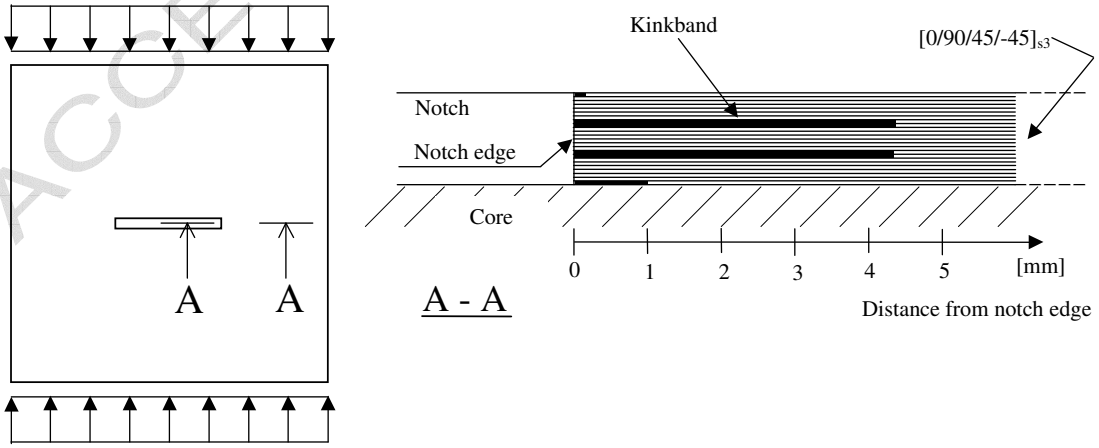

Figure 9. Sketch of kinkbands found in notched panel after interrupted loading, from [8].

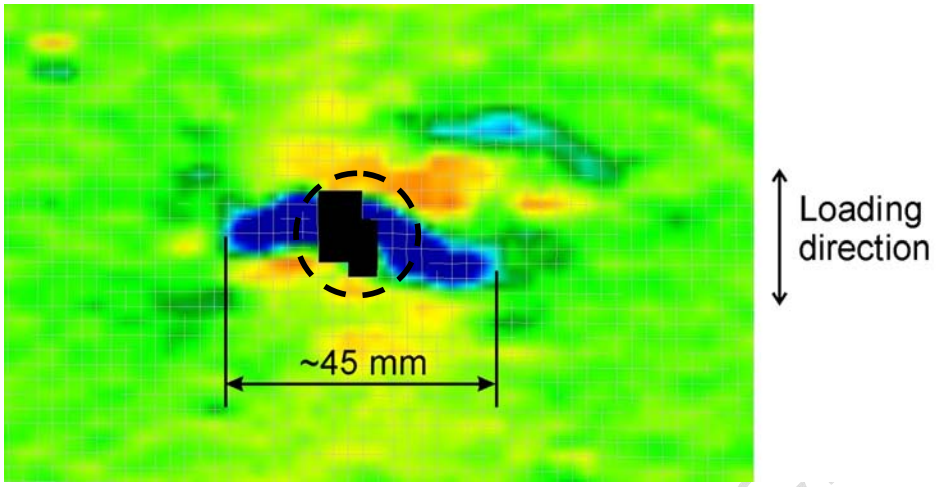

Figure 10. DSP image of longitudinal strain at load close to failure(ε_f=1%). The inscribed circle indicates the BVID overlapping delamination area.

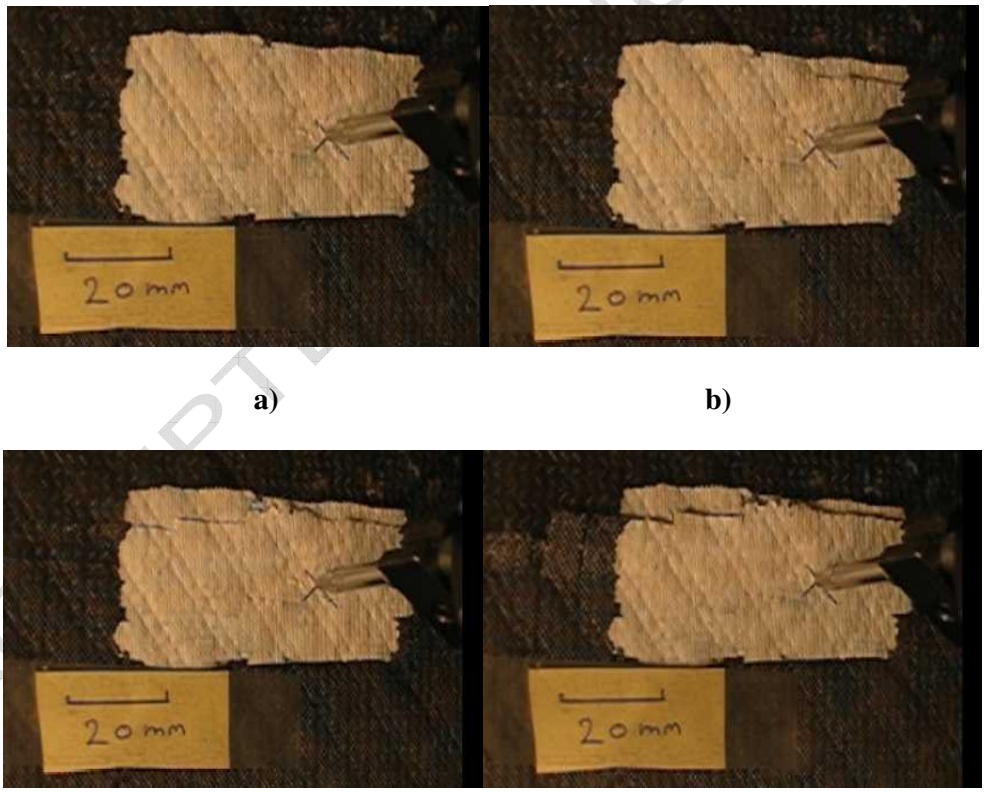

a) **b)**

c) **d)**

Figure 11 Damage formation in the surface ply at strains between approximately a) 0.45% to d) 0.48%. (The pointer seen centrally in the pictures is the dial gauge rod).

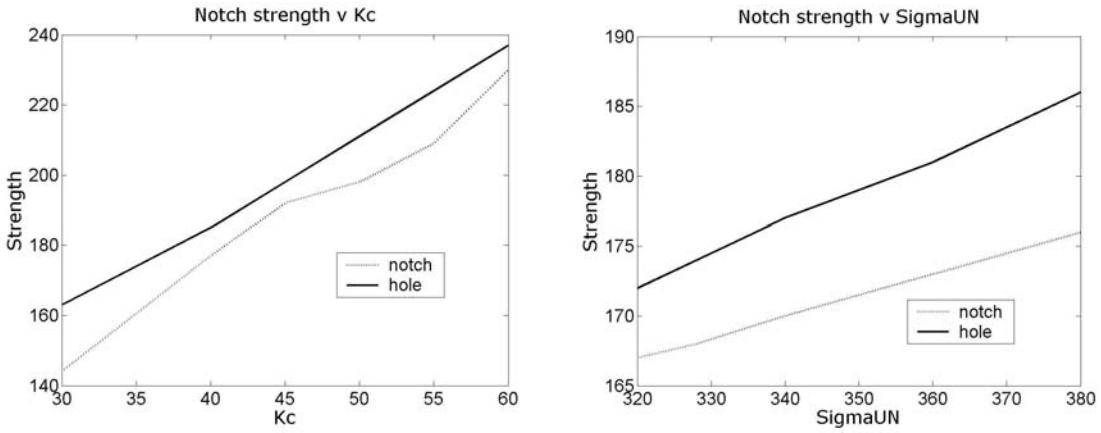

Figure 12 Sensitivity of the predicted notched compressive strength to changes in **a)** K_C (assuming σ_{un}=364.4MPa) and **b)** σ_{un}.(assuming K_C =39 MPa√m).

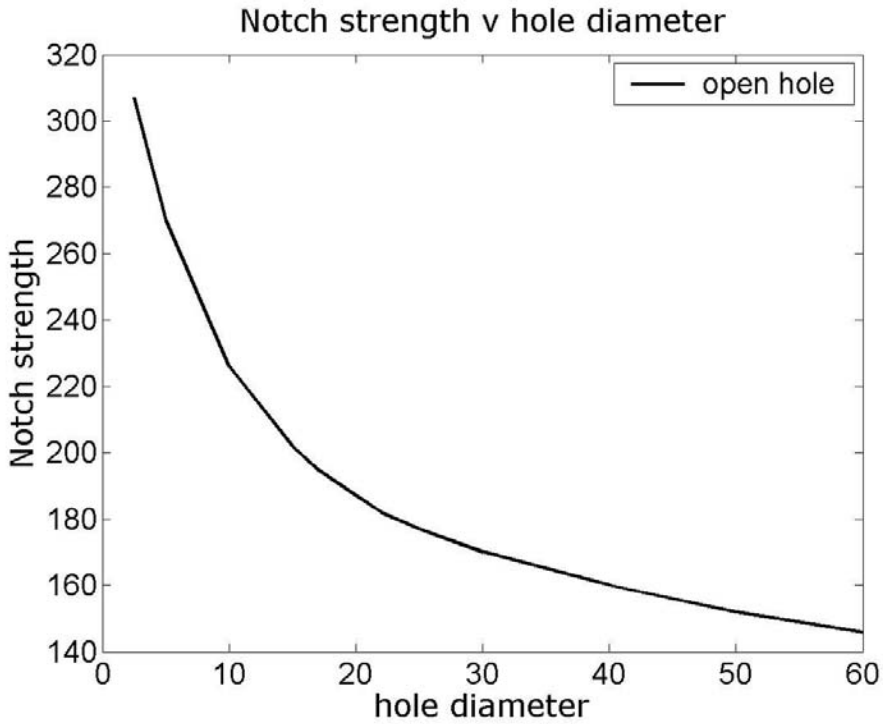

Figure 13 Notch strength predictions assuming an equivalent open hole, from Table 4.